

in late 1906, and a few angles were reobserved in 1925. These data, although fragmentary, are also consistent with 2 to 3 m of slip below 10 km. Most of the movements must then have occurred sometime between 1907 and 1925, but no further refinements on this time scale can be provided. The slip must have been predominantly aseismic, since seismic motion of 3 m over a 10-km depth interval and at least 70 km of fault (the distance from Point Arena to Fort Ross) would correspond (5) to an earthquake of at least magnitude 7, and no such event has occurred in this region since 1906.

The post-1906 observations suggest that strains for seismic faulting are not accumulated primarily by relatively continuous aseismic motion on the fault plane immediately below the seismic zone. Strain accumulation might be due to either steady or irregular motions on the fault plane at greater depths (say below about 30 km), in which case shear strains would be greatest at the fault trace and decrease away from it. Alternatively, the fault may be locked throughout the entire thickness of the lithosphere, with the San Andreas system loaded regionally by shear tractions applied far from the fault at the base or edges of the lithospheric plates. In this case, shear strains measured at the earth's surface by geodetic means would be approximately constant over a wide region on either side of the fault trace. A third alternative is that a "locked" section of the fault is loaded entirely by seismic or aseismic slip at its ends. It is also possible that strain is accumulated and released along many subsidiary subparallel faults as well as on the San Andreas itself. Each of these mechanisms produces a different pattern of surface deformation, and geodetic observations are potentially useful in differentiating between them. I consider that the data which have been examined to date are inconclusive in this regard, and thus the precise mode of strain accumulation remains an open question.

Some limited evidence from northern California does suggest irregular strain accumulation across the San Andreas fault in the half century before the 1906 earthquake. Astronomical azimuths, accurate to about 0.5 arc second, were observed in 1859, 1882, and 1907 between the primary triangulation stations Mount Diablo and Tamalpais (the second and third from north to south plotted in Fig. 1a) (6). This azimuth increased by

7.84 arc seconds in 1859 to 1882 and decreased by 0.55 arc second in 1882 to 1907, corresponding to relative right lateral motions parallel to the fault of +2.8 and -0.2 m, respectively. Reduction of the independent (though less accurate) triangulation network data gives changes of 5.38 and -1.57 arc seconds for essentially the same time intervals (6). The smaller change in the interval 1882 to 1907 is, at least in part, due to the elastic rebound that occurred in 1906, since station Tamalpais is only 15 km from the fault trace. The relative motion of 2.8 m during 1859 to 1882 far exceeds the rate since 1906 inferred from triangulation (4). An earthquake in 1868 on the Hayward fault, about 25 km from either station, appears too small to have contributed significantly to this large relative motion (7). Hence, these data, although limited, indicate some anomalous large crustal deformation away from the fault in the approximately 30 or more years preceding the 1906 earthquake.

The actual postseismic motions are probably more complex than indicated by this model of dislocation sources in a perfectly elastic half space. They should be understood as simple analog models which are convenient for discussion, and not necessarily realistic physical models of the actual time-dependent nonelastic processes. For example, a viscoelastic relaxation mechanism such as that proposed (8) to account for the vertical crustal movements which followed the thrust-type earthquake (magnitude, 8.2) in Nankaido, Japan, may be appropriate here.

Finally, the work reported here may have some relevance for the question

of whether large earthquakes cause secular shifts of the earth's rotational pole or excite the earth's Chandler wobble (9). Should large postseismic displacements be a common feature of strain release by great earthquakes, it seems likely that these aseismic movements would be more important than the earthquakes themselves in exciting the earth's polar motions.

WAYNE THATCHER

U.S. Geological Survey  
Menlo Park, California 94025

#### References and Notes

1. H. F. Reid, in *The California Earthquake of April 18, 1906, Report of the State Earthquake Investigation Commission* (Carnegie Institution of Washington, Washington, D.C., 1910), vol. 2, pp. 16-28.
2. Triangulation was carried out by the U.S. Coast and Geodetic Survey, now the National Geodetic Survey (NGS), and the observed direction lists have been made available to me by the courtesy of B. K. Meade of NGS.
3. G. Backus and F. Gilbert, *Geophys. J. R. Astron. Soc.* **16**, 196 (1968); *Phil. Trans. R. Soc. Lond. Ser. A Math. Phys. Sci.* **266**, 123 (1970); R. Wiggins, *Rev. Geophys. Space Phys.* **10**, 251 (1972); D. D. Jackson, *Geophys. J. R. Astron. Soc.* **28**, 97 (1972). The inversion methods described in these papers have been applied to geodetic data by W. Thatcher [*EOS Trans. Am. Geophys. Union* **54**, 1132 (1973)].
4. J. C. Savage and R. O. Burford, *J. Geophys. Res.* **78**, 832 (1973).
5. W. Thatcher and T. C. Hanks, *ibid.*, p. 8547.
6. J. F. Hayford and A. L. Baldwin, *The California Earthquake of April 18, 1906, Report of the State Earthquake Investigation Commission* (Carnegie Institution of Washington, Washington, DC., 1908), vol. 1, pp. 114-145.
7. Surface faulting was observed along 32 km of the Hayward fault, with right-lateral offsets varying from 25 to 90 cm (A. C. Lawson *et al.*, *ibid.*, p. 435).
8. A. Nur and G. Mavko, *Science* **183**, 204 (1974); H. Kanamori, *Annu. Rev. Earth Planet. Sci.* **1**, 213 (1973).
9. The question remains a controversial one; the spectrum of views is represented by: D. E. Smylie and L. Mansinha, *Geophys. J. R. Astron. Soc.* **23**, 329 (1971); M. Israel, A. Ben-Menahem, S. J. Singh, *ibid.* **32**, 219 (1973); F. A. Dahlen, *ibid.*, p. 203.
10. I thank J. C. Savage and A. H. Lachenbruch for helpful discussion.

8 March 1974

## Earthquake Mechanics in the Central United States

**Abstract.** *Focal mechanism solutions of earthquakes in the central United States suggest that local stress fields are important in determining the type and orientation of faulting. The implied stress system is considerably more complicated than that which would be produced by east-west trending compressive stresses, as previously suggested for this region.*

Sbar and Sykes (1) proposed a relatively simple stress model for the eastern portion of the North American continent. Using data obtained from geological observations, in situ stress measurements, and fault plane solutions, they concluded that the central United States is presently experiencing a predominantly horizontal compressive stress whose axis tends east-north-

east. A consequence of this model is that ongoing earthquake activity in this region should be mostly of the high-angle, thrust-type faulting with a strike in the north-south direction. However, a detailed investigation of moderate size earthquakes that occurred during the last 13 years within the area of Missouri, Kentucky, Tennessee, Illinois, Mississippi, and Arkansas indi-

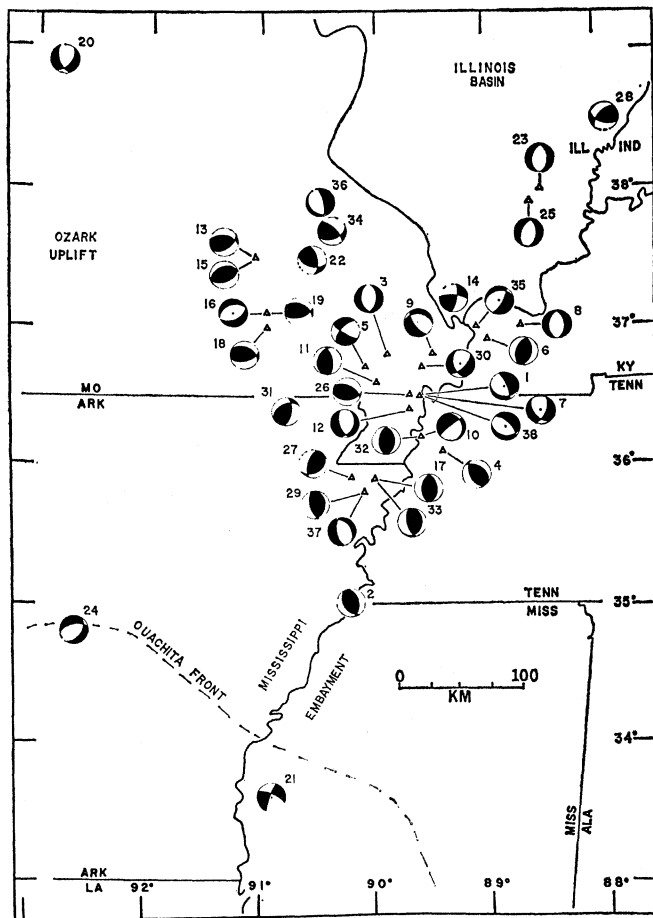


Fig. 1. Focal mechanisms in the central United States. The number beside each focal mechanism refers to the event listed in Table 1. The focal mechanisms are plotted by using an equal area stereographic projection; the black quadrants represent dilatational and the white quadrants compressional  $P$  wave first motion. The stereograph is centered at the epicenter, or, when offset for clarity, connected by an arrow with the epicenter indicated by a triangle.

Table 1. Focal mechanism parameters for earthquakes in the central United States; U.T., universal time. For event 15, see (5); for event 23, see (6).

Event	Date	Origin time (U.T.) (hr min sec)	Latitude ( $^{\circ}$ N)	Longitude ( $^{\circ}$ W)	Pressure axis		Tension axis	
					Trend (deg)	Plunge (deg)	Trend (deg)	Plunge (deg)
1	2 Feb 62	06 43 34.0	36.5	89.6	52	26	278	54
2	1 Jun 62	11 23 40.5	35.0	90.2	336	80	252	0
3	14 Jul 62	02 23 49.0	36.8	89.9	92	2	356	82
4	23 Jul 62	06 05 17.0	36.1	89.4	131	75	233	5
5	3 Mar 63	17 30 11.4	36.7	90.1	174	10	76	31
6	31 Mar 63	13 31 03.7	36.9	89.0	161	83	104	0
7	6 Apr 63	08 12 22.4	36.5	89.6	85	7	346	56
8	3 Aug 63	02 37 47.8	37.0	88.7	92	3	191	83
9	16 Jan 64	05 09 57.1	36.8	89.5	220	15	95	60
10	17 Mar 64	02 15 29.0	36.2	89.6	304	32	168	48
11	23 May 64	15 00 33.7	36.6	90.0	223	68	83	12
12	11 Feb 65	03 40 24.0	36.4	89.7	268	10	33	67
13	6 Mar 65	21 08 50.5	37.5	91.1	260	67	165	0
14	14 Aug 65	13 13 56.6	37.2	89.3	238	27	147	1
15	21 Oct 65	02 04 38.4	37.5	91.1	340	85	160	5
16	4 Nov 65	07 43 33.6	37.1	91.0	156	5	289	83
17	12 Feb 66	04 32 14.7	35.9	90.0	140	83	271	5
18	13 Feb 66	23 19 36.9	37.0	91.0	292	68	183	7
19	26 Feb 66	08 10 19.4	37.1	91.0	292	68	183	7
20	6 Dec 66	08 00 47.0	38.9	92.8	277	2	10	58
21	4 Jun 67	16 14 13.6	33.6	90.9	248	7	156	22
22	21 Jul 67	09 14 48.9	37.5	90.6	314	52	50	5
23	9 Nov 68	17 01 42.0	38.0	88.5	97	1	192	82
24	1 Jan 69	23 35 36.2	34.8	92.6	330	7	228	65
25	28 Feb 69	13 10 13.1	37.9	88.6	282	2	192	78
26	27 Mar 70	03 44 29.5	36.5	89.7	264	75	15	8
27	17 Nov 70	02 13 54.5	35.9	90.2	71	67	307	13
28	12 Feb 71	12 44 27.2	38.5	87.9	78	50	344	3
29	13 Apr 71	14 00 50.0	35.8	90.1	54	72	263	15
30	18 Oct 71	06 39 30.7	36.7	89.6	108	8	12	53
31	1 Feb 72	05 42 10.0	36.4	90.8	227	60	128	10
32	29 Mar 72	20 38 31.9	36.2	89.6	180	86	270	10
33	7 May 72	02 12 08.5	35.9	90.0	52	72	265	15
34	9 Jun 72	19 15 19.1	37.7	90.4	269	49	15	14
35	19 Jun 72	05 46 14.7	37.0	89.1	138	22	268	60
36	12 Jan 73	11 56 56.0	37.9	90.5	70	25	278	63
37	3 Oct 73	03 50 14.0	35.8	90.1	251	13	114	72
38	9 Oct 73	20 18 26.8	36.5	89.6	36	15	263	67

cates that such a simple regional stress model is not applicable.

Figure 1 illustrates focal mechanisms (2) determined for events listed chronologically in Table 1. The mechanism solutions were obtained by two independent methods—one using the sense of motion of crustal  $P$  phases ( $P_n$ ,  $P^*$ ,  $P_g$ ), and the other using the amplitude spectrum of the surface wave motion. Both methods employ seismicograms from Long Range Seismic Measurement (LRSM), the World Wide Standardized Seismic Network (WWSSN), the Canadian Network, Saint Louis University stations, and individual stations operated by the University of Missouri at Rolla, Indiana University, and the University of Arkansas. With the exception of events 1, 5, 14, 15, and 21 through 24, the indicated focal mechanisms were determined by the use of body wave data only. Thus, for the majority of events the mechanisms were determined from the sense of motion (compression or dilatation) of identifiable first and second  $P$ -phase arrivals (3). These compressions and dilatations were plotted on the lower hemisphere of an equal area stereographic projection at the appropriate azimuth and incidence angle. The strike and dip of the  $P$ -wave nodal planes were determined from a visual fit of the nodal planes to the available data. Depending on the particular event, we believe the errors in the strike and dip of the nodal planes are no more than  $10^{\circ}$  to  $20^{\circ}$ .

For the surface wave studies, source parameters for a hypothetical event are varied until the theoretical radiation patterns for Love and Rayleigh waves compare favorably with those actually observed. A constraint is that the chosen solution must be in reasonable agreement with the observed sense of motion of the various  $P$  phases. Errors in the strike and dip of the nodal planes, as determined by this method, are probably less than  $10^{\circ}$ . While this technique is superior to that which uses  $P$ -wave data only, it is restricted to events which excite fundamental modes of surface waves with periods in the range of 4 to 50 seconds sufficiently so that they are measurable on long-period seismicograms. Both the surface and body wave studies of this report, as well as other published and unpublished results, indicate that earthquakes in this region occur in the crust, at depths of 0 to 30 km.

The strike of the nodal planes shown in Fig. 1, with a few exceptions, can be grouped into two trends. The most

prominent is a nearly north-south strike for the group of earthquakes extending northward from Memphis, Tennessee, through latitude 38.5°N (events 2, 3, 6-8, 10-12, 17, 23, 25, 27, 29-33, and 35 in Fig. 1). However, along this trend there is a change from high-angle normal faulting south of 36.3°N to high-angle thrust faulting to the north. Thus, while there is a continuous trend of earthquake epicenters from Memphis to south-central Illinois, a tensional stress system predominates in the southern portion and a compressive stress system in the north.

The second grouping of nodal plane strikes (events 1, 4, 5, 9, 13, 15, 16, 18, 19, 22, 26, 34, and 38 in Fig. 1) consists of the southeast Missouri east-west trend, including the event of 21 July 1967, which has an approximate northwest-southeast strike. This suggests that the present stress distribution of this region is either controlled or significantly modified by the Ozark Uplift. At the junction of the two trends, near New Madrid, Missouri (36.5°N, 89.5°W), the indicated focal mechanisms require the stress distribution to be rather complex.

Two earthquakes, those of 1 June 1969 and 4 January 1967, are located on the Ouachita Front, which is described by Oetking (4) as being a thrust feature. Our data, although too few for us to conclude that the Ouachita Front is a compressive feature, do not disagree with such an interpretation. The earthquake of 1 January 1969 has a focal mechanism corresponding to a high-angle thrust fault, whose strike is similar to that of the Ouachita Front. The mechanism of the event of 4 July 1967 indicates a nearly vertical strike-slip character. Such a mechanism could result from the superposition of the thrust fault, compressive stress system associated with the Ouachita Front and a perpendicular normal fault, tensional stress system as found at Memphis. This hints at the possibility of tensional-type faulting extending southward from Memphis to the Ouachita Front. However, the present distribution of seismograph stations is inadequate to determine whether earthquakes are occurring along such an extension.

The results presented in this report bear on two important problems: the state of stress in the interior of a continental lithospheric plate, and the relation of present-day earthquake activity in the central United States to geological features. Concerning the

former problem, we find that on a localized scale the compressive stress distribution in the interior of a continental plate can be modified or significantly influenced by local features. In the central United States these features would include the Mississippi Embayment, the Ozark Uplift, and possibly the Ouachita Front (see Fig. 1). With regard to the latter problem, the focal mechanism solutions aid in identifying the active faults, and offer the potential of determining the extent of these fault systems. This information is essential for assessing the seismic risk at specific places, such as metropolitan areas and the sites of nuclear power plants, dams, and highway bridges.

RONALD L. STREET

ROBERT B. HERRMANN

OTTØ W. NUTTLI

Department of Earth and Atmospheric Sciences, Saint Louis University, Saint Louis, Missouri 63156

## Induced Polarization: A Geophysical Method for Locating Cultural Metallic Refuse

*Abstract. The problem of delineating cultural refuse sites (dumps) arises in civil engineering studies. Induced polarization measurements have been successfully applied in several cases. Laboratory tests on synthetic samples indicate that the effect is due to the metal content of the dumps. The method may be applicable to archeological investigations.*

The induced polarization (IP) method of geophysical prospecting has been in use since about 1948 (1) and has been applied principally to the exploration of deposits of metallic minerals (2).

The IP method makes use of the observation that the electrical impedance of metallic minerals is a function of the frequency of the electrical current used in the measurement. The conductivity increases with the frequency (3). Measurements of the impedance

### References and Notes

1. M. I. Sbar and L. R. Sykes, *Geol. Soc. Am. Bull.* **84**, 1861 (1973).
2. Tabulated data for focal mechanisms based solely on the sense of motion of crustal *P* phases can be found in R. L. Street, thesis, Saint Louis University, in preparation. Data for events 1, 5, 14, 15, and 21 through 24 can be found in R. B. Herrmann, thesis, Saint Louis University, in preparation.
3. Focal mechanisms based only on *P*-wave data vary in quality, depending on the number of data points available. The well-determined events had approximately 35 *P*-phase polarities. All the earthquakes of Table 1 are in this category except for numbers 6, 7, 18, 20, 25, 29, 32, and 34 through 37, for which only about 15 points were available per earthquake.
4. P. Oetking, compiler, *Geological Highway Map of the Mid-Continent, No. 1* (American Association of Petroleum Geologists, Tulsa, Okla., 1966).
5. B. J. Mitchell published a solution based on surface wave data which differs only slightly from that given here [*J. Geophys. Res.* **76**, 886 (1973)].
6. W. Stauder and O. W. Nuttli have previously published a focal mechanism for the event of 9 November 1968 [*Bull. Seismol. Soc. Am.* **60**, 973 (1970)].
7. We acknowledge discussions with W. Stauder concerning the focal mechanism solutions. Supported by NSF grant GA-40595 and AFOSR contract F44620-73-C-0042.

17 January 1974; revised 11 March 1974

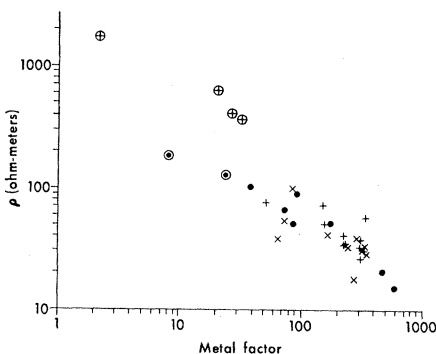


Fig. 1 (left). Resistivity plotted against metal factor measured at several sites. The location code is (●) Bedford (8), (×) Lexington (9), and (+) Acton (10). Circled points were measured off the dump site in an adjacent region. Fig. 2 (right). Histogram of frequency effect (FE) measured on landfill and dump sites. The average value is 8 percent. The location code is the same as in Fig. 1.

function are made in either the frequency or the time domain (4).

In metallic mineral deposits, the conduction of electricity occurs along two kinds of paths. One is made up of connected pore spaces containing pore fluids (5). The other is similar to this but it also includes some proportion of metallic minerals along its "length." At each interface in the latter where a boundary occurs between a metallic mineral and the surrounding pore fluid,

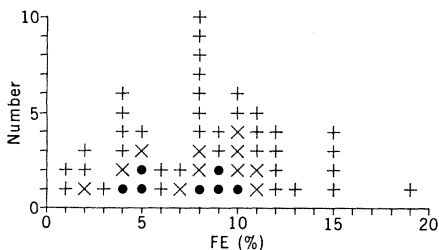


Fig. 2 (right). Histogram of frequency effect (FE) measured on landfill and dump sites. The average value is 8 percent. The location code is the same as in Fig. 1.